Biomaterials 32 (2011) 6982–6994

Contents lists available at ScienceDirect

Biomaterials

journal homepage: www.elsevier.com/locate/biomaterials

Galactosylated cellulosic sponge for multi-well drug safety testing

Bramasta Nugraha [a,b], Xin Hong [b,c], Xuejun Mo [b,d], Looling Tan [b], Wenxia Zhang [c], Po-Mak Chan [b,c], Chiang Huen Kang [b], Yan Wang [b,e], Lu Thong Beng [f], Wanxin Sun [g], Deepak Choudhury [a,b], Jeffrey M. Robens [i], Michael McMillian [h], Jose Silva [h], Shannon Dallas [h], Choon-Hong Tan [d], Zhilian Yue [b], Hanry Yu [a,b,c,i,j,k,*]

[a] NUS Graduate School for Integrative Sciences and Engineering, Centre for Life Sciences, #05-01, 28 Medical Drive, Singapore 117576, Singapore
[b] Institute of Bioengineering and Nanotechnology, A*STAR, The Nanos, #04-01, 31 Biopolis Way, Singapore 138669, Singapore
[c] Department of Physiology, Yong Loo Lin School of Medicine, National University Health System, MD9-03-03, 2 Medical Drive, Singapore 117597, Singapore
[d] Department of Chemistry, Faculty of Science, National University of Singapore, S05-03-09, 3 Science Drive 3, Singapore 117576, Singapore
[e] Department of Hepatobiliary Surgery, Zhujiang Hospital, Southern Medical University, 5101280, PR China
[f] Electron Microscopy Unit, Yong Loo Lin School of Medicine, National University of Singapore, MD5-01, 12 Medical Drive, Singapore 117597, Singapore
[g] Bruker Nano Surface, the Helios, #10-10, 11 Biopolis Way, Singapore 138667, Singapore
[h] Johnson and Johnson, Pharmaceutical Research and Development, Drug Safety Sciences, Raritan, NJ, USA
[i] Mechanobiology Institute, T-Labs, #05-01, 5A Engineering Drive 1, Singapore 117411, Singapore
[j] Singapore-MIT Alliance, Computational and System Biology Program, E4-04-10, 4 Engineering Drive 3, Singapore 117576, Singapore
[k] Singapore-MIT Alliance for Research and Technology, 3 Science Drive 2, S16-05-08, Singapore 117543, Singapore

ARTICLE INFO

Article history:
Received 6 May 2011
Accepted 28 May 2011
Available online 8 July 2011

Keywords:
Cellulose
Galactose
Hydrogel
Sponge
Cytochrome P450
Drug induction

ABSTRACT

Hepatocyte spheroids can maintain mature differentiated functions, but collide to form bulkier structures when in extended culture. When the spheroid diameter exceeds 200 μm, cells in the inner core experience hypoxia and limited access to nutrients and drugs. Here we report the development of a thin galactosylated cellulosic sponge to culture hepatocytes in multi-well plates as 3D spheroids, and constrain them within a macroporous scaffold network to maintain spheroid size and prevent detachment. The hydrogel-based soft sponge conjugated with galactose provided suitable mechanical and chemical cues to support rapid formation of hepatocyte spheroids with a mature hepatocyte phenotype. The spheroids tethered in the sponge showed excellent maintenance of 3D cell morphology, cell–cell interaction, polarity, metabolic and transporter function and/or expression. For example, cytochrome P450 (CYP1A2, CYP2B2 and CYP3A2) activities were significantly elevated in spheroids exposed to β-naphthoflavone, phenobarbital, or pregnenolone-16α-carbonitrile, respectively. The sponge also exhibits minimal drug absorption compared to other commercially available scaffolds. As the cell seeding and culture protocols are similar to various high-throughput 2D cell-based assays, this platform is readily scalable and provides an alternative to current hepatocyte platforms used in drug safety testing applications.

1. Introduction

Spheroids are three-dimensional multi-cellular aggregates that exhibit a high degree of cell-to cell contact. Compactness of cells contained in 3D spheroids *in vitro* preserve complex *in vivo* cell phenotypes which are otherwise absent in conventional 2D cultures [1,2]. 3D multi-cellular spheroids have been useful in multiple applications including stem cell, cancer biology and tissue engineering research [3–6]. In 3D hepatocyte spheroids, tight cell–cell junctions help sustain cell viability for extended culture periods and maintain high level liver-specific functions e.g. albumin secretion, urea synthesis and cytochrome P450 activity [7,8]. These attributes make 3D hepatocyte spheroids potentially attractive for *in vitro* drug safety testing.

Growing spheroids using previously described methods such as by hanging drop, centrifugation, on 2D substrates, or in suspension culture are limited since these methods provide no means of physical spheroid constraint during extended culture. Consequently there is difficulty in controlling spheroid size and in

* Corresponding author. Department of Physiology, Yong Loo Lin School of Medicine, National University Health System, MD9-03-03, 2 Medical Drive, Singapore 117597, Singapore. Tel.: +65 65163466; fax: +65 68748261.
E-mail address: hanry_yu@nuhs.edu.sg (H. Yu).

0142-9612/$ – see front matter © 2011 Elsevier Ltd. All rights reserved.
doi:10.1016/j.biomaterials.2011.05.087

manipulating floating spheroids for cell-based drug safety testing applications [9–12]. When smaller spheroids collide to form larger spheroids in culture, mass transfer of oxygen, nutrients, metabolites and drugs can be impeded in the inner core yielding high variability during drug safety testing [11]. Attempts to constrain 3D spheroids in a diffusible dimension have been achieved by growing spheroids on microfabricated platforms [13,14], polyurethane foams [15,16], and polymeric scaffolds [17], but these methods do not provide the optimal chemical and mechanical microenvironments needed to maintain high level cellular functions. Furthermore, scalability in manufacturing and simplicity in operation for high-throughput, large-scale drug safety testing applications is also problematic.

To address these concerns we have constrained hepatocyte spheroids in a macroporous network of a soft galactosylated cellulosic sponge. The macroporosity of the sponge provides control over spheroid size while the conjugated galactose ligands present chemical cues to the cells to form spheroids. The soft hydrogel-based sponge would be proper to maintain mature hepatocyte differentiated functions via control of the matrix rigidity [18]. The configuration of the sponges supports high-throughput applications and ease of use, similar to readily available 2D culture platforms. Sponges are fabricated in bulk and sliced thin to minimize drug absorption. Hepatocyte spheroids grown in the sponge can maintain 3D cell morphology, cell–cell interactions, polarity, transporter expression, excretion and metabolic functions; and exhibit in some cases improved CYP450s enzyme activities.

2. Materials and methods

2.1. Materials

All chemicals and reagents were purchased from Sigma Aldrich (Singapore), unless otherwise stated.

2.2. Chemical synthesis of galactosylated hydroxypropyl cellulose allyl (HA Gal)

Hydroxypropyl cellulose (HPC), Mw = 80,000 g/mol and ~3.4 ° of etherification was dehydrated by azeotropic distillation in toluene. 4 g of dried HPC was dissolved in anhydrous chloroform (100 mL), to which 2.095 mL allyl isocyanate 98% and 1 mL dibutyltin dilaurate 95% were added dropwise. The mixture was stirred vigorously for 48 h at room temperature, after which it was precipitated in an excess amount of anhydrous diethyl ether. Following vacuum drying, the product was dissolved in deionized water (DI H_2O), purified by dialysis for 3 days, and finally lyophilized to the intermediate product, hydroxypropyl cellulose allyl (HA). For galactose conjugation, 1 g of HA was dissolved in 15 mL anhydrous dimethylformamide (DMF) in which the hydroxyl groups were activated by addition of 1,1′-carbonyldiimidazole (0.322 g in 2 mL DMF). D-(+)-galactosamine HCl (0.427 g in 30 mL DMF), which was dissolved with addition of triethylamine, was added to the mixture with two folds molar ratio compared to D-(+)-galactosamine HCl. The reaction was carried out for a further 48 h at room temperature. To remove impurities, the mixture was further dialyzed in excess methanol and subsequently in deionized water for 3 days each and the final product (hydroxypropyl cellulose allyl galactose, HA Gal) was lyophilized. A schematic diagram with the complete synthesis described, including ^{1}H NMR characterization is shown in Fig. 1C.

2.3. Preparation of HA Gal sponges

HA Gal was dissolved in deionized water to a final concentration of 7.5% wt/vol after which the solution was inserted into tubes (diameter 6 mm, length 3 cm). The tubes were heated in a water bath (50 °C) until phase separation occurred, and then crosslinked by γ irradiation for 30 min at a dose of 10 kGy/h (Gammacell 220, MDS Nordion, Canada). The sponge monoliths were obtained by breaking tubes subsequent to freezing in dry ice. A Krumdieck tissue slicer (Alabama Research & Development USA) was used to cut the sponge uniformly (50 rpm for 1 mm thickness). We fabricated thin sponge slices to reduce possible drug absorption during assays. Sliced sponges were washed extensively with excess amounts of deionized water for 3 days to remove uncross-linked polymers. Finally, slices were lyophilized and sterilized by γ irradiation (1.7 kGray total dose) prior to cell seeding with hepatocytes. A schematic diagram of the sponge preparation is described in Fig. 1B.

As a comparison, galactosylated polyethylene terephthalate (PET Gal) membranes were also seeded with hepatocytes. Preparation and synthesis steps of PET Gal membranes have been described previously [11].

2.4. Physiochemical characterization of HA Gal sponges

2.4.1. High performance liquid chromatography elution assay

Galactose presence in the sponge was detected by a HPLC elution assay. Sponges were hydrolyzed by 6 N HCl at 110 °C for 24 h. Cooled hydrolyzed solutions were evaporated, re-suspended in 500 μL deionized water and derivatized using the ATTO-TAG™ CBCQA amine-derivatization kit (Molecular Probes, USA) for fluorescence detection on a C-18 column using HPLC (Agilent Technology, place). The mobile phase consisted of A) water +0.1% trifluoroacetic acid (TFA), and B) acetonitrile + 0.1 %TFA with an A/B gradient 98:2/70:30 in 45 min. The flow rate was 1 mL/min and the fluorescence detector settings were excitation at 450 nm, and emission at 550 nm.

2.4.2. X-Ray photoelectron spectroscopy

X-Ray photoelectron spectroscopy was used to qualitatively verify galactose ligand conjugation onto the HA chemical backbone. Measurements were made on a VG ESCALAB Mk II spectrometer with a MgKa X-ray source (1253.6 eV photons) at a constant retard ratio of 40.

2.4.3. Elastic modulus measurement

The elastic modulus of the sponge was measured by atomic force microscopy (Bioscope Catalyst, Veeco Instruments, Santa Barbara, CA) in deionized water. A hybrid Atomic Force Microscopy (AFM) probe consisting of a silicon nitride cantilever and a silicon tip (ScanAsyst-Fluid, Veeco Probes, Camarillo, CA) was used. The deflection sensitivity was calibrated by ramping force-distance curves on a glass surface, and the spring constant was calibrated by the thermal noise method. After calibration, 128 × 128 force-distance curves were recorded over an area of 5 μm × 5 μm by force volume. Each force-distance curve was analyzed by fitting to the Hertz model with conical tip geometry and Poisson ratio of 0.5. The obtained elastic moduli from each force-distance curve were mapped into a bitmap image with 128 × 128 pixels. The curve fitting and statistical analysis was implemented by a self-developed Fortran program (available upon request). The relationship between elastic modulus with the measured force is described as $F = 2/\pi \cdot E/1 - \nu^2 \tan \alpha \delta^2$, where F is the measured force, E is Young's elastic modulus, ν is the Poisson ratio of the material under measurement (0.5 was used in the data processing), α is the half angle of the probe (22 °) and δ is the sample deformation.

2.4.4. Zeta potential measurement

HA Gal solutions in deionized water with different concentrations (0.125–2.5 % wt/vol) were heated to 50 °C to let the phase separation occur. The zeta potentials were measured using Malvern Zeta Sizer Nano ZS 90 (Malvern Instruments, United Kingdom) normalized to the base potential of water.

2.4.5. Scanning electron microscopy

Top and cross section views of the sponge surface morphology and porosity were captured using SEM (JEOL JSM-5600, Japan) at 10 kV. High magnification of SEM (15,000 folds) was performed to observe the sponge surface structure. Prior to imaging, the dried sponge was sputter-coated with platinum for 60 s. Pore size distribution of the sponges was quantified with ImageJ software (version 1.43u) from collective SEM top view images of the sponges.

2.5. Hepatocyte isolation and culture

Hepatocytes were isolated from male Wistar rats weighing 250–300 g using a modified *in situ* collagenase perfusion method [19]. Animals were handled according to the IACUC protocols approved by the IACUC committee of National University of Singapore. Cells were maintained with Williams' *E* medium supplemented with 10 mM $NaHCO_3$, 1 mg/mL BSA, 10 ng/mL of EGF, 0.5 mg/mL of insulin, 5 nM dexamethasone, 50 ng/mL linoleic acid, 100 units/mL penicillin, and 100 mg/mL streptomycin and were incubated with 5% CO_2 at 37 °C and 95% humidity. Medium was replenished every two days. Viability of hepatocytes was determined to be >90% by the Trypan Blue exclusion assay. Yields were approximately 10^8 cells per rat. Freshly isolated rat hepatocytes (10^5 cells in 10 μL culture medium) were loaded to the centre of the wells in 48-well plates; the sponges were immediately inserted into the wells to allow cells to be absorbed into the sponges from the lower surface. Another aliquot of 10^5 cells in 10 μL culture medium was then seeded into the sponge by dropping the cell suspension onto the top sponge surface. The cell suspension was absorbed into the sponge interior due to the inherent hydrophilicity of the sponges. The process takes 10 min to 1 h. Fresh culture medium was added to the sponge edge (300 μL per sponge in 48-well plate). Hepatocytes seeded on a collagen sandwich platform (0.29 mg/mL collagen concentration) were used as control as reported previously [20].

2.6. Hepatocyte spheroids characterization

2.6.1. Spheroids size distribution

Spheroid size distribution was quantified using ImageJ software from phase contrast images of living hepatocyte spheroids cultured on the PET galactose membrane and in the HA Gal sponges on day 1, 3 and 6.

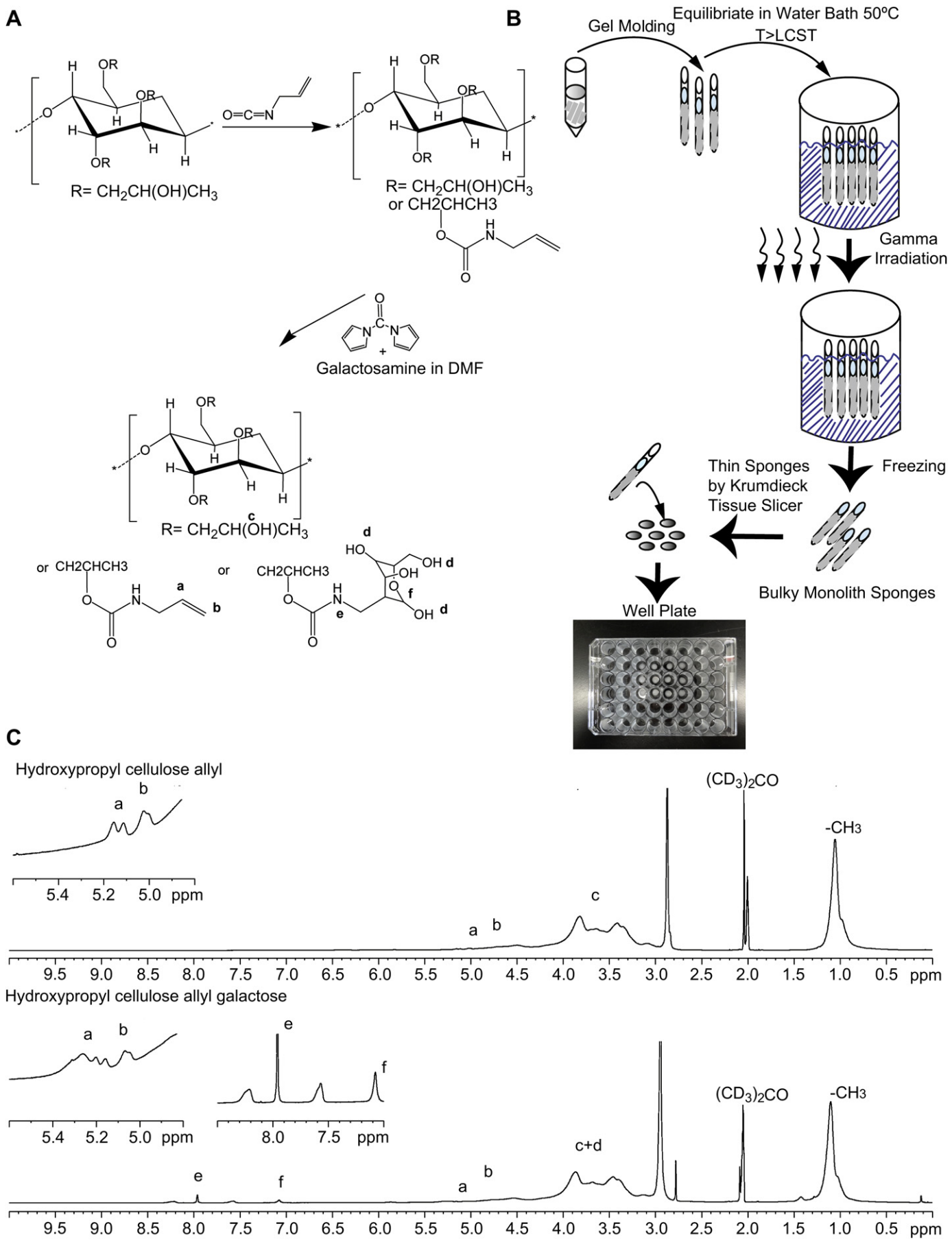

Fig. 1. Materials synthesis. A) Chemical synthesis steps, B) Schematic diagram of galactosylated cellulosic sponge preparation and C) 1H NMR spectrum of galactosylated cellulosic sponge in d_6-acetone.

2.6.2. Scanning electron microscopy

Hepatocyte spheroids in sponges on day 1, day 3 and day 7 were fixed with 2.5% glutaraldehyde overnight and stained with 1% OsO_4 for 1 h. Samples were then dehydrated step-wise with ethanol (25%, 50%, 75%, 90% and 100%) for 10 min each, dried in a vacuum oven and sputter-coated with platinum for 60 s. The samples were viewed with a scanning electron microscope (JEOL JSM-5600, Japan) at 10 kV.

2.6.3. Live/dead staining

Hepatocytes spheroids were co-stained with Cell Tracker Green (CTG, 20 μM) (Molecular Probes, USA) and Propidium Iodide (PI, 25 μg/mL) (Molecular Probes, USA) to quantify live and dead cells, respectively. Cells were incubated for 30 min at 37 °C and then fixed with 3.7% paraformaldehyde for 30 min at room temperature. Fluorsave (Merck Chemicals) was applied to the stained spheroids to minimize photo-bleaching. Images were acquired by confocal laser scanning microscopy (Zeiss LSM510, Germany) at 488 and 543 nm excitation wavelengths.

2.6.4. Time-lapse imaging of spheroids formation

The dynamic process of hepatocyte spheroid formation in the sponges was monitored immediately upon cell seeding. Hepatocytes were pre-stained with 20 μM Cell Tracker Green (Molecular Probe, USA) for 20 min prior to seeding. Cell-seeded sponges were imaged consecutively for 12 h using a DeltaVision system (Applied Precision, USA) equipped with nano-positioning and a controlled temperature chamber set at 37 °C and 5% CO_2. Images were acquired in hourly intervals to minimize light exposure to the cells.

2.7. Hepatocyte functional assessments

2.7.1. Immunofluorescence microscopy

To stain F-actin, E-cadherin and Mrp2/CD147, hepatocytes cultured for 48 h in the sponges were fixed in 3.7% paraformaldehyde for 30 min. For staining F-actin, the cells were permeabilized for 5 min in 0.1% Triton X-100 and incubated with 1 μg/mL TRITC-phalloidin (Molecular Probes, USA) for 20 min. For E-cadherin, the cells were permeabilized with 0.1% Triton X-100 for 30 min, blocked with 1% BSA for 30 min, incubated with mouse anti-rat E-cadherin (BD, USA) overnight at 4 °C followed by incubation with a FITC conjugated anti-mouse secondary antibody (Santa Cruz, USA). For MRP2/CD147 staining, the cells were permeabilized with 0.1% Triton X-100 for 30 min, blocked with 1% BSA for 30 min, incubated with rabbit anti-rat MRP2 (Sigma Aldrich, Singapore) and mouse anti-rat CD147 (Serotec, USA) overnight at 4 °C and eventually incubated with FITC conjugated anti-mouse and TRITC conjugated anti-rabbit secondary antibodies (Sigma–Aldrich, Singapore). For all stained samples, Fluorsave (Merck Chemicals) was applied to minimize laser-induced photo-bleaching. Microscopy images were acquired with 20× lens on a Zeiss Meta 510 upright confocal microscope. The 3D image stack was reconstructed using LSM Browser.

2.7.2. Transmission electron microscopy

Hepatocyte spheroids in sponges were fixed with 3.7% paraformaldehyde for 30 min and treated with 1% OsO_4 for 2 h at room temperature. Samples were subsequently dehydrated step-wise with ethanol (25%, 50%, 75%, 95% and 100%) for 10 min followed by 100% acetone twice for 20 min each. Upon dehydration, samples were then treated with 1:1 ratio mixture of acetone and araldite resin for 30 min at room temperature followed by overnight treatment at a 1:6 ratio at room temperature. On the following day, the samples were placed into araldite resin for 30 min at room temperature before transferring into a 40 °C oven for another 30 min. Araldite resin was subsequently changed followed by 1 h treatments at 45 °C and 1 h at 50 °C. Lastly, the samples were embedded with araldite resin at 60 °C for 24 h. Sections of 90–100 μm thickness were sliced using a Leica EM UC6 Ultramicrotome, collected onto 200-mesh copper grids and co-stained with uranyl acetate and lead citrate for 10 min each. Observation was undertaken with a Transmission Electron Microscope (TEM) (JEOL JEM-1010, Japan) at voltage 100 kV.

2.7.3. Biliary excretion of fluorescein dye

For monitoring the functional status of hepatocyte repolarization, we visualized the excretion of fluorescein dye via bile canaliculi. Hepatocytes spheroids were incubated with 15 μg/mL fluorescein diacetate (Molecular Probes, USA) in culture medium at 37 °C for 45 min at different time intervals (16 h, 24 h and 48 h) post-seeding. The cultures were then rinsed and fixed with 3.7% paraformaldehyde for 30 min before viewing with a 20× lens on a Zeiss Meta 510 upright confocal microscope.

2.7.4. Albumin secretion & urea synthesis

Albumin secretion by hepatocytes on days 1, 3, 5 and 7 were assayed using a rat albumin enzyme-linked immunosorbent assay quantitation kit (Bethyl Laboratories Inc., Montgomery, Texas). Urea synthesis by cultured hepatocytes in culture medium spiked with 1 mM NH4Cl for 90 min was assayed on the same days using a Urea Nitrogen Kit (Stanbio Laboratory, Boerne, Texas). All functional data were normalized by the number of cells seeded in the sponges which was quantified using the Quant-iT™ PicoGreen dsDNA Assay Kit (Invitrogen, Singapore).

2.8. Drug inducibility of hepatocyte spheroids

2.8.1. Reverse transcriptase polymerase chain reaction

RNA was extracted from hepatocytes cultured as 3D spheroids in HA Gal sponges by TRIzol (Invitrogen, Singapore). Total RNA concentration was quantified by a Nanodrop (Thermo scientific) and 1 μg of RNA was converted to-cDNA by High Capacity RNA-to-cDNA kit (Applied Biosystems). Primers were designed using Primer 3 and real-time PCR was performed by using SYBR Green fast master mix in an ABI 7500 Fast Real-Time PCR system (Applied Biosystems). Gene expression was calculated using the ΔΔCT method normalized to GAPDH. The primers used in experiment are shown below. These basal level gene expression experiments were performed on day 3 and day 5 post-seeding, which were the day intervals for the induction experiments.CYPs

Gene	Forward sequence	Reverse sequence
CYP1A2	CACGGCTTTCTGACAGACCC	CCAAGCCGAAGAGCATCACC
CYP2B2	TCTCACAGGCACCATCCCT	GTGGGTCATGGAGAGCTG
CYP3A2	TGGGACCCGCACACATGGACT	TCCGTGATGGCAAACAGAGGCA
CYP4A1	TCATGAAGTGTGCCTTCAGC	GATGTTCCTCACACGGGAGT
CYP2E1	AGGCTGTCAAGGAGGTGCTA	ATGTGGGCCCATTATTGAAA
Transporters		
Mdr1a	TGACATTCGCTCTCTTAACAT	TGGGATTCCGTATGAGG
Mrp2	CGCGAGGAGAGCATTAT	GGCAAGGTAGAATTTGGTTAT
Ntcp	CATTATCTTCCGGTGCTATGA	GTTTCTGAGCATCGGGATT
Bsep	TGACATTCGCTCTCTTAACAT	TGGGATTCCGTATGAGG
Oatp1	CTTAAAGCCAACGCAAGACC	AGAGATACCCAAGGGCACAA

Mdr1a: Multi-Drug Resistance 1a, Mrp2: Multi-drug Resistance Protein 2, Ntcp: Na/taurocholate Co-transporting Polypeptide, Bsep: Bile Salt Export Pump, Oatp1: Organic Anion Transporting Polypeptide 1.

2.8.2. CYP450 induction study

Hepatocyte spheroids cultured in sponges were used to study drug induction of three CYP450 enzymes, i.e. CYP1A2, CYP2B2 and CYP3A2. 72 h post-seeding, cells were incubated at 37 °C with culture medium containing inducers (50 μM β-naphthaflavone, for CYP1A2; 1 mM phenobarbital, for CYP2B2; 50 μM pregnenolone-16α-carbonitrile, for CYP3A2). After 48 h of induction, medium was removed and the cells were further incubated for 2 h at 37 °C with Krebs-Henseleit-bicarbonate (KHB) buffer (118 mm NaCl, 1.2 mM $MgSO_4$, 1.2 mM KH_2PO_4, 4.7 mm KCl, 26 mM $NaHCO_3$, and 2.5 mM $CaCl_2$) containing the P450 substrates (200 μM phenacetin, for CYP1A2; 200 μm bupropion, for CYP2B2; and 5 μM midazolam, for CYP3A2). The drug metabolite product in the supernatant was assayed from induced and vehicle (0.1% DMSO) treated hepatocytes cultured in HA Gal sponges or in collagen sandwich cultures. Detected metabolite products for CYP1A2, CYP2B2 and CYP3A2 were acetaminophen (APAP), hydroxy bupropion (OH-bupropion) and hydroxy midazolam (OH-midazolam), respectively. Cell supernatants (300 μL) were added with 50 μL internal standards (100 ng/mLAPAP-D4 for APAP and 1′–OH–midazolam, 100 ng/mL OH-bupropion-D6 for OH-bupropion) and dried in a vacuum concentrator (Eppendorf). The obtained residues were reconstituted in 50 μL methanol containing 0.1% formic acid and centrifuged at 12,000 g for 10 min. The supernatants were then analyzed by Liquid Chromatography-Mass Spectrometry (LC-MS Finnigan LCQ Deca XP Max, Agilent 1100 series). The LC-MS experimental setup consisted of solvent A, 0.1% formic acid in water, and solvent B, 0.1% formic acid in methanol, with a flow rate of 0.8 mL/min; and a Phenomenex Onyx-monolithic C-18 column with dimensions of 100 × 3.0 mm. The mass spectrometry parameters were spray voltage 5 kV, sheath gas flow rate of 80 arbitrary unit, auxiliary gas flow rate set at 20 arbitrary unit, capillary temperature of 350 °C, tube lens 45 V, and capillary voltage 30 V. Elution schemes for the three different metabolites products were for APAP and OH-midazolam, solvent B gradually increased from 6% to 90% in 6 min while for OH-bupropion, solvent B gradually increased from 10% to 90% in 6 min.

2.9. Drug absorption properties of sponge

Sponges were incubated with various hydrophobic and hydrophilic drugs (with different net charges) dissolved in PBS for 24 h at 37 °C. The concentrations of each compound before and after incubation were recorded with UV Spectrophotometer (Shimadzu, Japan). Percentage of drug absorption was determined by the formula as follows:

$$\%\text{Absorption} = \left(1 - \frac{\text{Concentration}_{\text{Final}}}{\text{Concentration}_{\text{Initial}}}\right) \times 100\%$$

2.10. Statistical analysis

Statistical comparisons were undertaken using paired two-tailed Student *t* tests. Results are expressed as mean ± standard error of the mean.

3. Results

3.1. Synthesis and characterization of galactosylated cellulosic sponge

The first step in the chemical synthesis of the macroporous cellulosic sponges involved the conjugation of allyl groups onto hydroxypropyl groups of hydroxypropyl cellulose to act as cross-linking sites during γ irradiation, as described elsewhere [21]. The galactose conjugation onto the remaining available hydroxypropyl groups was performed using 1,1′-carbonyldiamidazole in anhydrous dimethylformamide (Fig. 1A). The sponge fabrication is depicted in detail in Fig. 1B.

Galactose presence on the chemical backbone was verified by ^{1}H NMR by identifying additional peaks at ~7–8 ppm which indicates additional bonds from the attached galactose (Fig. 1C). The integrated peak area between 2.5 ppm and 5 ppm showed an increase from 2.067 to 2.402 relative amount of the proton, which correlated to the presence of more hydroxyl groups from the conjugated galactose (estimated to be 1 conjugated galactose per 3 subunits of the HA Gal backbone).

To further confirm the presence of galactose in the sponges, we hydrolyzed the sponges with 6 N hydrochloric acid at 110 °C for 24 h, derivatized using an amine-derivatization kit and analyzed the products using HPLC. As a comparison, a pure D-(+)-galactosamine sample was also assayed. One eluted peak in the HPLC chromatogram at ~43 min represents the bound galactose (Fig. 2A) [11]. An X-ray photoelectron spectroscopy spectrum showed increased nitrogen atomic counts after conjugation (~1.5% increase) (Fig. 2B). Lectin conjugated with FITC was also used to specifically stain galactose on the sponge surface and showed increased FITC signal, compared to non-galactose containing HA sponges (data not shown).

Surface morphology and porosity of the sponges were characterized using SEM. Image analysis of the sponge porosity showed the average pore size to be between 110 and 130 μm (Fig. 2C) for potentially constraining cellular spheroids within diffusion-limited dimension [22,23]. Measurement of the elastic modulus of the sponges using atomic force microscopy revealed an average modulus of 5.6 kPa (Fig. 2D). This modulus is considered to be soft and close to the modulus of native rat and human livers [24,25]. The net charge of the HA Gal structure in deionized water was measured through zeta potential measurement of the HA Gal at different concentrations ranging from 0.125 to 2.5% wt/vol (Fig. 2E). At 2.5% wt/vol the value approached an almost neutral charge (−0.91 mV), which at concentrations beyond 2.5% wt/vol the solution became difficult to measure accurately due to its high viscosity. Therefore, at the working concentration for cell culture (7.5% wt/vol), the value is considered to be a neutral net charge.

In addition to the macroporous structure viewed from the top of the sponges, the porosity also expanded throughout the sponges in cross-sectional areas (Fig. 2F i,ii). High magnification images of the sponge surface revealed surface nano-roughness in the nanometer scale which might tether the hepatocyte spheroids to the sponge (Fig. 2F iii). The dry sponge was incubated in fluorescein isothiocyanate solution to stain the sponge's macroporous structure in aqueous phase. By laser confocal microscopy, we observed that the macroporosity was maintained as a hydrated macroporous network structure in an aqueous environment (Fig. 2F iv) in contrast to typical hydrogels that lose their porosity in an aqueous environment.

3.2. Characterization of hepatocyte spheroids in cellulosic sponges

3.2.1. Hepatocyte spheroids formation in cellulosic sponges

Rat hepatocytes cultured on three different platforms revealed platform-dependent cell behaviors (Fig. 3A). Hepatocytes cultured on collagen monolayers were relatively flat and spread on day 3 onwards, which correlate with rapid loss of differentiated functions [11]. Hepatocyte spheroids formation on galactosylated polyethylene terephthalate membranes (2D PET Gal membrane) took 3 days to form, and often collided with adjacent spheroids to form larger spheroids. In the HA Gal sponge cultures, hepatocytes immediately organized into 3D spheroids within 1 day of culture, and maintained similar sizes until at least day 6. Hepatocyte spheroids formed in the HA Gal sponges were smaller than those formed on 2D PET Gal membrane, with spheroid diameter 60.7 ± 15.9 μm and 108.1 ± 19.2 μm, for each platform, respectively. In addition, spheroids formed in HA Gal sponges were constrained by the sponge pores and thus did not easily detach as those plated on 2D PET Gal membranes.

Hepatocyte spheroids cultured between day 1 and 7 showed gradual increases in surface smoothness and disappearance of the cell–cell boundaries (Fig. 3B). On day 1, the cell morphology was spherical. The nature of the hydrophilic and soft hydrogel sponges would prevent the cells from spreading, which normally occurs on hard substrates [18]. Tethered spheroids on the sponge surface was observed (Fig. 3B). The arrows in the figure show the contact points where the spheroids adhere to the sponge surface.

Hepatocyte spheroid viability, which was assessed by co-staining live and dead cells using Cell Tracker Green (CTG) and Propidium Iodide (PI), respectively, showed no PI signal which revealed good viability maintenance from day 1 to day 7 in culture (Fig. 3C). The CTG signals illustrated indistinguishable borders between single cells in the spheroids, which reflected the tightness of the cell–cell contacts.

Dynamic observation of hepatocytes upon seeding into the sponges for the first 12 h showed that by 7 h, the cells had reorganized themselves into hepatocyte spheroids with no further detectable changes in cell movement (Fig. 3D). The spheroid morphology appeared compact and with cell boundaries becoming indistinguishable after 7 h.

3.2.2. Hepatocyte spheroids phenotypes in cellulosic sponges

Immunofluorescence staining of F-actin, E-cadherin and MRP2/CD147 in the hepatocyte spheroids 48 h post-seeding, in comparison to collagen sandwich control, showed localization of these markers (Fig. 4A). As would be expected in non-spreading cells, F-actin staining revealed that the actin cytoskeleton had a predominant cortical localization in both sponge and collagen sandwich cultures and an absence of stress fibers. E-cadherin staining, a marker of cell–cell junctions demonstrated that cells in the hepatocyte spheroids have tight associations between neighboring cells. E-cadherin expression also supports the maintenance of cell viability during long-term culture [26]. MRP2/CD147 staining marked the apical and basolateral domains of the hepatocytes, respectively. In MRP2/CD147 staining image (Fig. 4A rightmost panel), the signals showed a comparable and non-colocalized signal as observed in collagen sandwich culture.

Ultrastructural views observed by transmission electron microscopy illustrated the sub-cellular micro-structures located inside the spheroids. The images of hepatocyte spheroids cultured for 48 h demonstrated a space between neighboring cells, reminiscent of the bile canaliculi with the presence of microvilli (Fig. 4B) [27,28]. Tight junctions between the two cells were also clearly observed.

3.2.3. Hepatocyte spheroids differentiated functions in cellulosic sponges

Several hepatocyte functions are thought to be dependent on the polarized phenotype of the cells, including biliary excretion, albumin secretion and urea synthesis. Since we observed an early

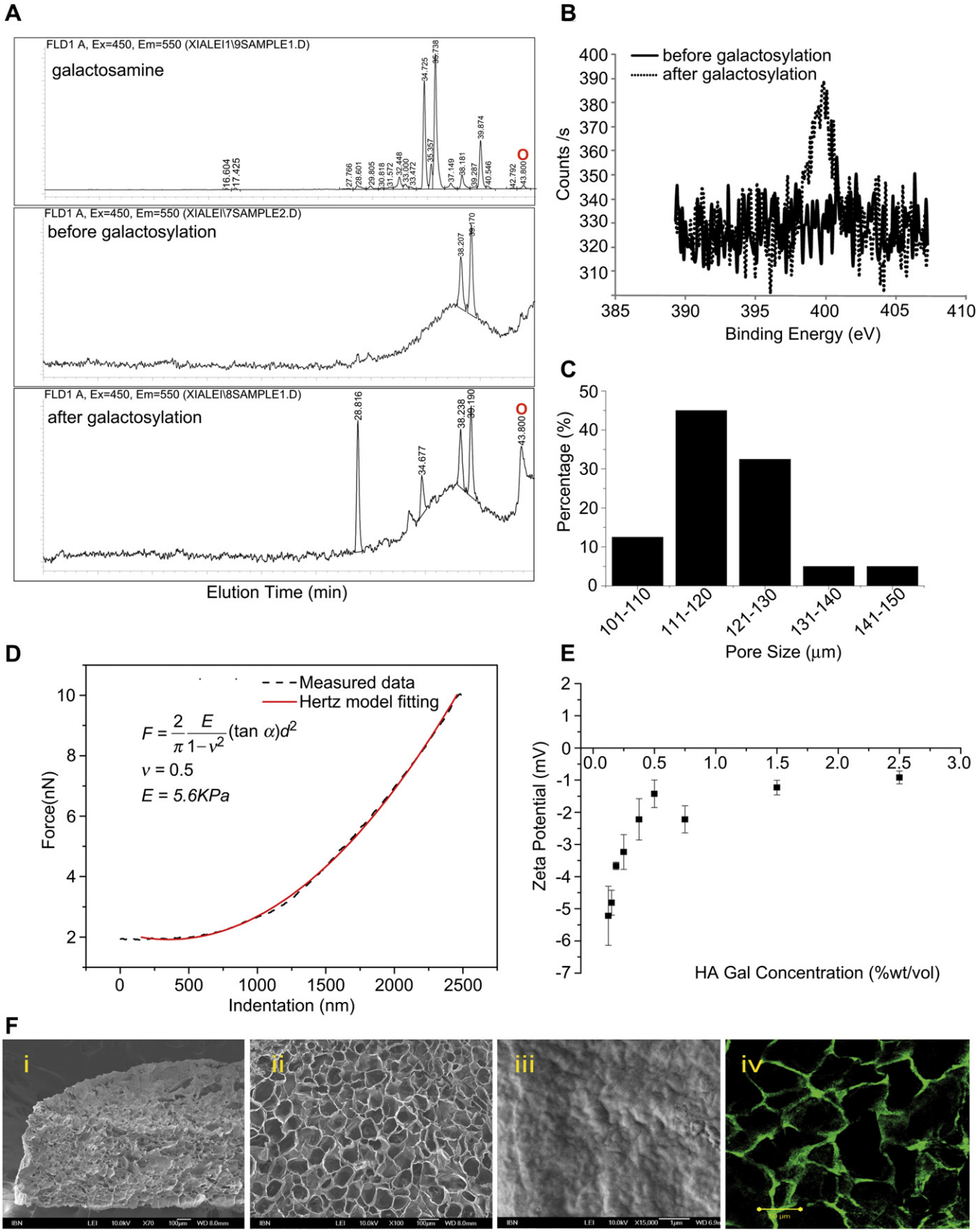

Fig. 2. Characterizations of cellulosic sponge. A) Galactose elution assay with High Performance Liquid Chromatography (HPLC), B) X-ray Photoelectron Spectroscopy, C) Sponge pore size distribution, D) Elastic modulus measurement by Atomic Force Microscope (AFM), E) Zeta potential measurement, and F) Secondary Electron Image of sponge: I) Cross section view (scale bar 100 μm), ii) Top view (scale bar 100 μm), iii) Sponge surface nano-roughness (scale bar 1 μm) and iv) Confocal image of FITC stained sponge (scale bar 50 μm).

appearance of polarity markers of hepatocytes in the cellulosic sponges, we investigated whether these functions were also enhanced.

Biliary excretion was examined by the addition of fluorescein diacetate dye at various time intervals, including 16, 24 and 48 h post-seeding (Fig. 4C). Polarized hepatocytes formed bile canaliculi structures between neighboring cells that contain the MRP2 transporter (see Fig. 4A). Viable cells in the spheroids will cleave FDA into fluoroscein dye by intracellular esterases which then be excreted by MRP2 into the bile canaliculi. FDA staining in the hepatocyte spheroids formed in the sponge showed an accumulation in the bile canaliculus between two cells, starting from 16 h post-seeding, significantly faster than has been reported in collagen sandwich which normally occurs between 48 and 72 h post-seeding [29]. Morphology of the FDA signal resembled the mouth-like shape of bile canaliculi described elsewhere [30,31], confirming its proper excretion.

Maintenance of albumin secretion and urea synthesis, markers of mature differentiated hepatocytes, during extended culture is a prerequisite for drug safety testing applications [32]. Fig. 4D demonstrates that these functions were generally better maintained in hepatocytes cultured in the HA Gal sponge compared to the collagen sandwich for at least 7 days. When the hepatocytes were cultured in collagen sandwich, they had albumin secretion rate ranging from 57.74 μg/million cells/day to 219.70 μg/million cells/day for 7 days of culture. Hepatocytes cultured in the sponge on average secreted albumin at the rate ranging from 127.51 μg/million cells/day to 1145 μg/million cells/day, showing their peak on day 5 (Fig. 4D left panel). There was a decrease of secretion to 908.95 μg/million cells/day on day 7. Urea synthesis in sponge-cultured hepatocytes increased from day 1 (71.31 μg/million cells/90 min) to day 7 of culture (666.44 μg/million cells/90 min; Fig. 4A right panel). On average, hepatocytes cultured in collagen sandwich showed relatively stable and lower urea synthesis rate in the range of 30.52 μg/million cells/90 min to 40.52 μg/million cells/90 min.

3.2.4. Hepatocyte spheroids drug-metabolizing enzymes and transporters maintenance

Maintenance of drug-metabolizing enzymes (CYP1A2, CYP3A2, CYP4A1, CYP2B2 and CYP2E1) and drug transporter expression (Mdr1a, Mrp2, Ntcp, Bsep and Oatp1) was examined in hepatocyte spheroids and compared to sandwich culture. Hepatocyte spheroids showed higher expression of CYP1A2, CYP3A2 and CYP4A1 than the hepatocytes cultured in collagen sandwich (Fig. 5A left panel). The expression of CYP2B2 on day 5 was similar for both culture configurations. For CYP2E, collagen sandwich culture slightly outperformed the hepatocyte spheroids culture on day 3; however on day 5, the spheroid culture showed a 3.42 folds higher expression of CYP2E than in collagen sandwich.

In addition to drug-metabolizing enzymes, various drug transporters known to be expressed in liver were analyzed. These transporters are involved in the influx of endogenous substances and xenobiotics into liver, or conversely the efflux of endogenous substances and xenobiotics into the bile or blood [33]. Together with CYPs, these transporters mediate clearance of drugs from liver. Bsep, Mdr1a, and Mrp2 are efflux transporters which are present on the apical canalicular membrane [34,35]. Oatp1 and ntcp are located in the basolateral membrane and act as influx transporters. On day 3 and 5 in culture, we observed a modest upregulation of Mrp2 in the hepatocyte spheroids at 2.6 folds and 1.7 fold, respectively (Fig. 5A). On day 3, Oatp1 had similar expression in hepatocytes cultured in both culture configurations. On day 5, however, there was a drastic upregulation (13 folds) in the sponge culture. Mdr1a expressions for both culture configurations were similar for both days 3 and 5. For both Ntcp and Bsep expression on both day 3 and day 5, hepatocyte spheroids exhibited lower level expression than the collagen sandwich culture.

For all three cytochrome P450s in the drug induction experiments, the basal levels in the sponge-cultured hepatocyte spheroids showed higher metabolite production than the collagen sandwich (Fig. 5B–D). This reflected an improved ability of hepatocyte spheroids in metabolizing drugs and correlated with the upregulation of drug-metabolizing enzyme expression in hepatocyte spheroids at basal level (Fig. 5A left panel). Metabolite production CYP1A2 induced hepatocyte spheroids showed a higher absolute amount than the hepatocytes in collagen sandwich, 4973 ± 1327 ng/million cells per 2 h and 1449 ± 173 ng/million cells per 2 h, respectively, as well as a higher fold of metabolite production activity between induced and basal levels, 18.67 folds for spheroids versus 6.66 folds for collagen sandwich (Fig. 5B). For CYP2B2 induction, induced hepatocyte spheroids and collagen sandwich exhibited an absolute value of metabolite production of 73.91 ± 1.90 ng/million cells per 2 h and 43.96 ± 7.18 ng/million cells per 2 h, respectively, but reflecting a similar 4.53 and 4.64 folds change over basal levels in both culture configurations (Fig. 5C). For CYP3A2 induction, the absolute value of metabolite production of the induced spheroids culture showed a lower value than collagen sandwich culture, 139.85 ± 9.14 ng/million cells per 2 h and 541.38 ± 132.83 ng/million cells per 2 h, respectively (Fig. 5D). This translated into a 6.53 and 31.98 folds induction over basal levels for each of the culture configurations. The 6.53 folds induction of metabolic activity for CYP3A2 over basal levels is still considered significant.

3.3. Drug absorption properties comparison of cellulosic sponge and other commonly used scaffolds

To be useful in drug safety testing it is important to characterize absorption of different classes of commonly used drugs in the sponge platform. Eight drugs with differing hydrophilicity and net charges were chosen. The definition of hydrophobic and hydrophilic drugs was determined based on drug partition coefficients (log P), where hydrophobic drugs have log $P >> 0$ and hydrophilic drugs have $P \leq 0$. For comparison, drug absorption experiment was performed with three other scaffolds for hepatocyte culture *in vitro*, i.e. collagen gel, PuraMatrix™ gel, and Reinnervate polystyrene scaffolds [6,36,37]. The drug absorption properties of two tested hydrophobic drugs were found to be dependent on the solubility limit of each drug (Fig. 6). Testosterone with low water solubility (23.4 μg/mL) and bulky chemical structure was found to be severely absorbed by all four tested scaffolds. WY14643, another hydrophobic drug with higher water solubility (40 μg/mL), showed 9%, 14%, 24% and 0% drug absorption to the HA Gal sponge, collagen gel, PuraMatrix™ gel and Reinnervate scaffold, respectively. For the hydrophilic drugs with positive and negative charges, HA Gal sponge absorbed at most 10% of the tested drugs, which was less than the collagen gel and PuraMatrix™ gel but more than Reinnervate scaffold. Hydrophilic drugs with neutral net charges such as nicotine and caffeine were 29% and 19% absorbed in the HA Gal sponge, respectively. This was comparable to the extent of adsorption by collagen gels, 23% and 29%, respectively. PuraMatrix™ gel absorbed 45% and 32% of nicotine and caffeine, respectively. Reinnervate scaffold absorbed 5% and 11% of nicotine and caffeine, respectively. The significant absorption of hydrophilic drugs with neutral net charges to the sponge correlated with the net neutral charge of the sponge (shown by its Zeta potential in Fig. 2E). In most of the tested drugs for drug absorption, the HA Gal sponge outperformed the collagen

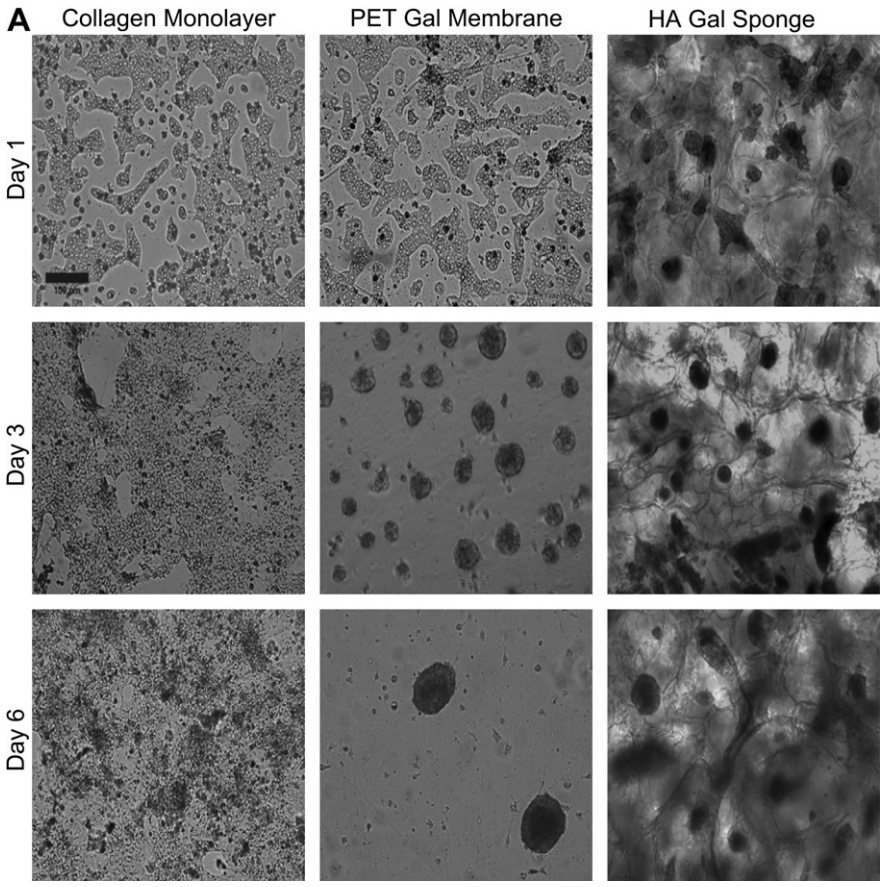

Fig. 3. Hepatocyte spheroids formation in cellulosic sponge. A) Rat hepatocyte cultured in 3 different platforms. Scale bar is 100 μm. Diameter of hepatocyte spheroids formed on PET Gal membrane on day 3: 39.8 ± 8.1 μm, day 6: 108.1 ± 19.2 μm, and in HA Gal sponge day 1: 46.1 ± 9.3 μm, day 3: 55.7 ± 21.1 μm, day 6: 60.7 ± 15.9 μm, B) SEM Images of hepatocyte spheroids formed in HA Gal sponge. Arrow in the tethered spheroid figure indicates the tethering location of the spheroid on sponge surface. C) Hepatocyte spheroids viability, D) Time-lapse images of hepatocyte spheroids formation in HA Gal sponge.

sandwich, which is the commonly used biomatrix for hepatocyte culture.

4. Discussion

We have conjugated galactose ligands onto cellulosic sponges by using D-(+)-galactosamine, which is commercially available, more cost effective and readily useful for large-scale synthesis than customized 1-O-(6-aminohexyl)-D-galactopyranoside (AHG), which has been used previously [11,38,39]. The absence of a hexyl spacer in galactosamine compared to AHG was found only critical in the early stage of cell attachment kinetics, as shown by the comparison of HepG2 cells adhesion energy on the polyethylene membrane conjugated with AHG and lactobionic acid [40]. Unlike other hydrogels, the macroporous networks in our cellulosic sponge support the *in situ* formation and maintenance of polarized hepatocyte spheroids [41–43]. The cellulosic sponge, which acts as a hepatocyte substratum anchor, did not prevent cell aggregation, as would normally happen in cell culture platforms with excessive extracellular matrix presentation [44]. In addition, galactose presented chemical cues to the hepatocytes to reorganize into 3D spheroids, while the macroporous structure constrained and tethered them physically. Since the galactose ligand only interacts weakly with ASGPR receptors in the hepatocyte cell membrane [11], it is the combination of the physical and chemical cues in the sponge which is important in establishing stable constrained hepatocyte spheroids.

Cellulosic sponges were fabricated in large-scale with thin dimensions to reduce drug absorption. Compared to other scaffolds used for cultivation of hepatocyte spheroids, our sponge has a softer mechanical stiffness ($E < 10$ kPa) [37,45], durable macroporosity and is fabricated without chemical cross-linkers, yet crosslinked through stable chemical bonds [21]. The soft stiffness of the sponge will prevent cell spreading, which is important for maintenance of the mature hepatocyte phenotypes [18].

Hepatocytes cultured as 3D spheroids in the cellulosic sponge were tethered onto the sponge surface, which has nano-roughness, and constrained within the macroporosity of the sponge. Hepatocyte spheroids started to form at 7 h post-seeding with a gradual increase in cell boundary tightness. They exhibited maintenance of cell viability for 7 days in culture, polarity markers and 3D cell morphology including a cortical F-actin cytoskeleton and tight cell–cell junctions. At 16 h post-seeding they have excreted fluorescein dyes into bile canaliculi-like structures, which was faster than the other platforms used to form hepatocyte spheroids or collagen sandwich cultures [12,29,46]. These translated into high level of albumin secretion and urea synthesis, which were significantly higher than collagen sandwich culture. Compared to other galactosylated scaffolds used for culturing primary rat hepatocytes, hepatocytes cultured in cellulosic sponges also showed relatively higher maintenance of albumin

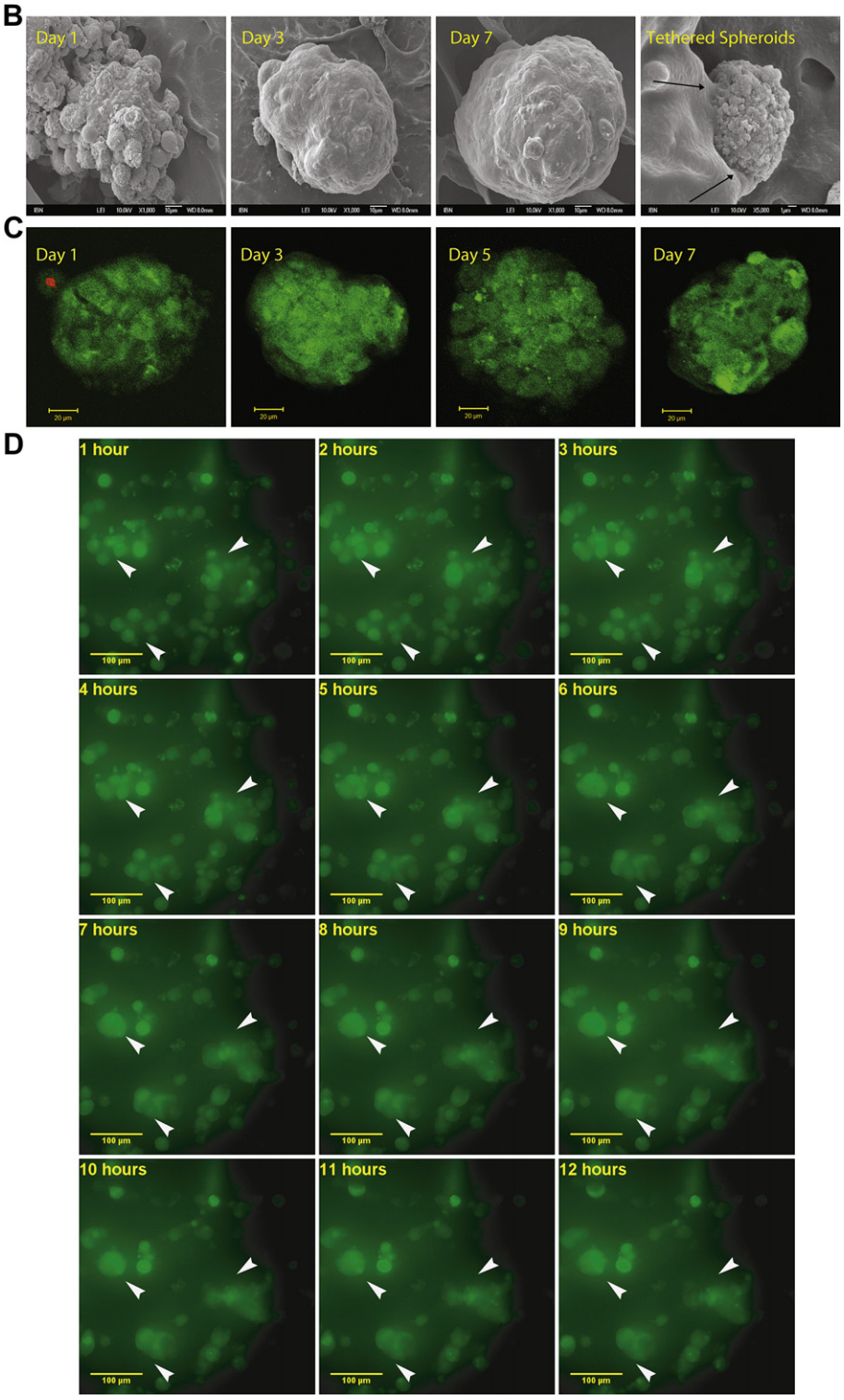

Fig. 3. (*continued*).

secretion and urea synthesis at least two fold [47–49]. Hepatocyte spheroids constrained in the sponge expressed multiple phase 1 CYP450 enzymes and drug transporters at the same or higher level than hepatocytes cultured in collagen sandwich with the exception of Ntcp and Bsep.

When these spheroids were incubated with known P450 inducers such as β-naphthoflavone (CYP1A2), phenobarbital (CYP2B2), or pregnenolone-16α-carbonitrile (CYP3A2), the absolute value of metabolite production of CYP1A2, CYP2B2 and CYP3A2 were elevated, respectively. Levels of drug metabolites

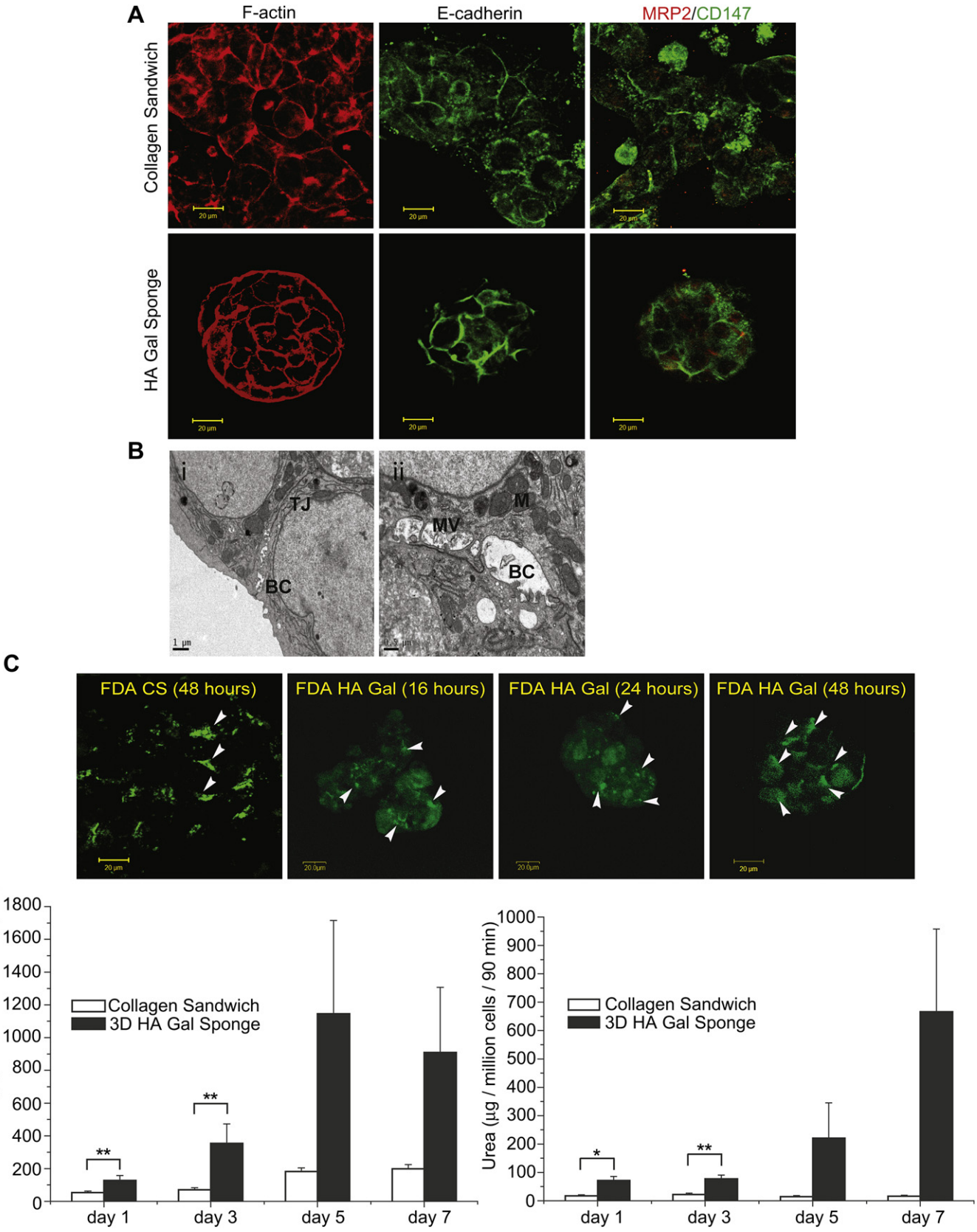

Fig. 4. Cellular characterizations of hepatocyte spheroids. A) Immunofluorescence of mature hepatocyte markers (scale bar 20 μm), B) Transmission Electron Microscopy images at 48 h post-seeding (scale bars for i and ii are 1 μm and 0.5 μm, respectively. TJ: Tight Junction, BC: Bile Canaliculi, Mv: Microvili, M: Mitochondria), C) Fluorescein diacetate excretion of hepatocytes in collagen sandwich (CS) and sponge (HA Gal) at different time intervals (scale bar 20 μm), D) Albumin secretion and urea synthesis function of hepatocyte in the sponges and collagen sandwich. $^{**}p$ value < 0.05 and $^{*}p$ value < 0.1.

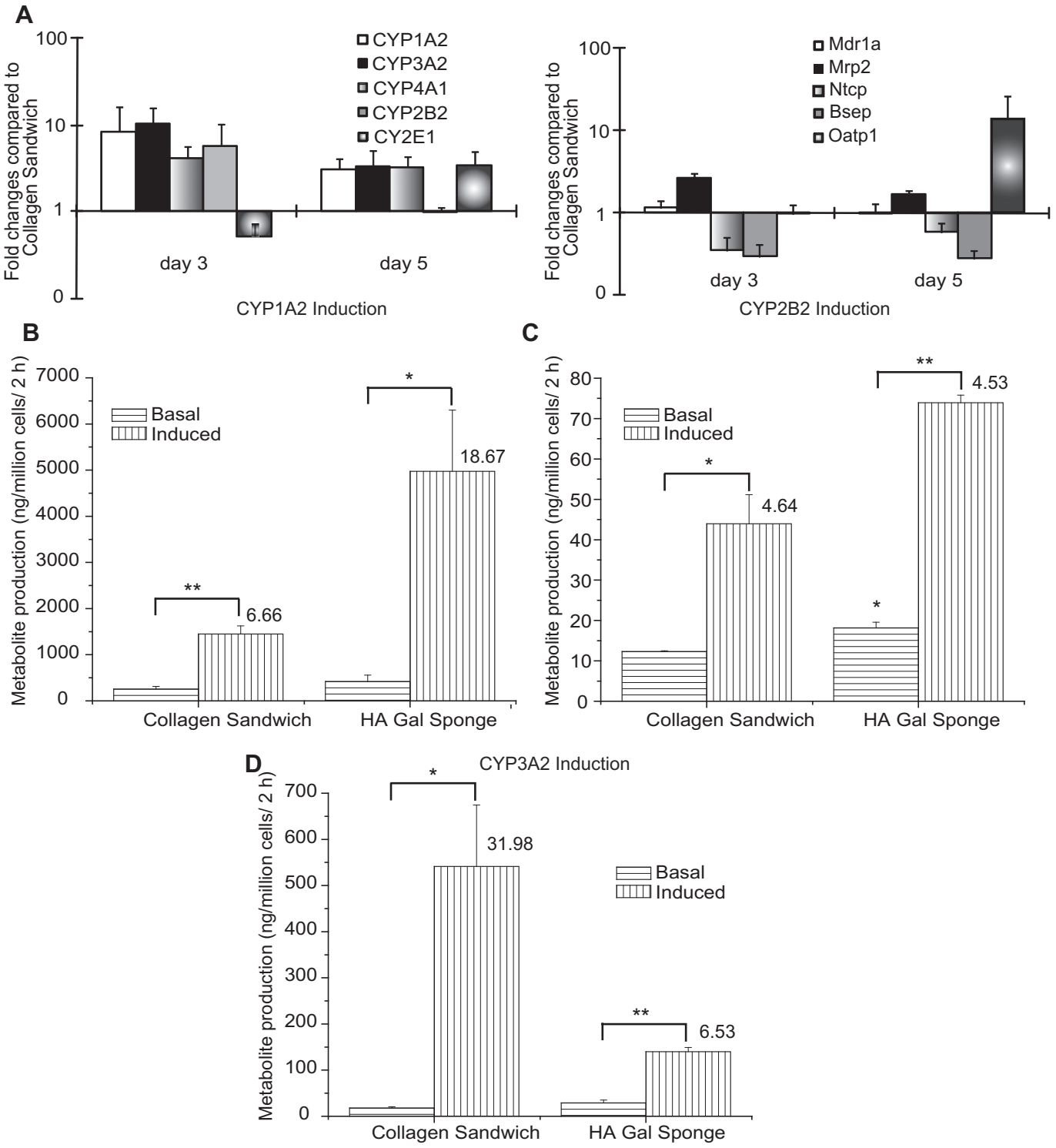

Fig. 5. Metabolic responses to drugs. A) Basal level gene Expression of CYP450s enzymes and drug transporters, B-D) Drug induction of CYP1A2, CYP2B2 & CYP3A2 (numbers on top of induced level bar denote fold induction activity changes, $^{**}p$ value < 0.05 and $^{*}p$ value < 0.1).

under basal conditions, as measured by LC/MS, in the hepatocyte spheroids cultured in the sponge were higher compared to the collagen sandwich (Fig. 5B–D). Upon drug inductions, the amount of metabolites increased even more in the hepatocytes cultured in HA Gal sponge, while only true for CYP1A2 and CYP2B2, the major CYPs in rat hepatocytes [50–52]. Similar induction folds of CYP2B2 in sponge and collagen sandwich culture were correlated to the reduction of CYP2B2 expression in hepatocyte spheroids between day 3 and day 5 to a similar level with the collagen sandwich culture on day 5 (Fig. 5A left panel). CYP3A2 showed lower but still significant level of induction. The sponge exhibited lower or comparable drugs absorbency than collagen gel, Puramatrix™ gel and Reinnervate scaffold. Overall, the galactosylated cellulosic sponge supports the uniform formation,

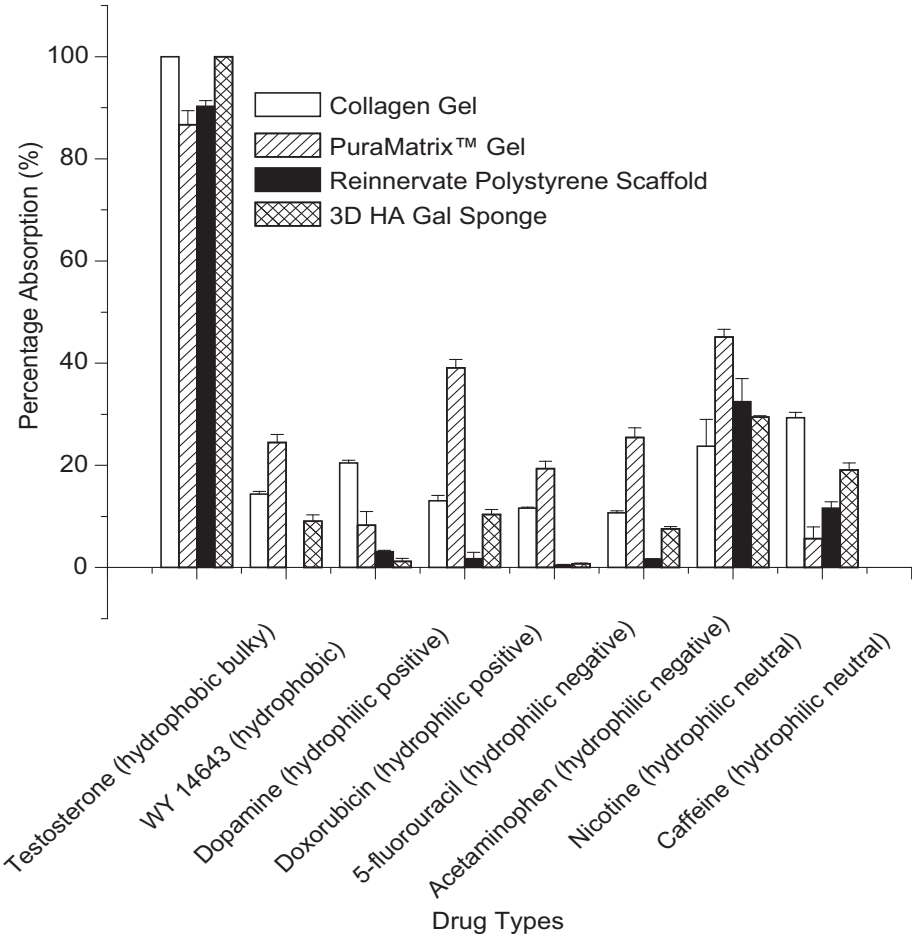

Fig. 6. Drug absorption properties of cellulosic sponge compared to other commercially available scaffolds. Percentage absorption for each drug is quantified as the maximum drug absorption after 24 h incubation with the scaffolds.

maintenance and functions of hepatocyte spheroids that are useful for drug safety testing.

5. Conclusion

We have synthesized and fabricated a galactosylated macroporous cellulosic hydrogel sponge as a platform to culture hepatocytes as 3D spheroids for drug safety testing applications. The soft macroporous cellulosic sponge with conjugated galactose facilitates the formation of hepatocyte spheroids by presenting both the mechanical cues (via matrix rigidity) and chemical cues for the hepatocytes to reorganize into 3D spheroids within 7 h post-seeding. The constrained hepatocyte spheroids maintain cell viability, cell polarity markers, and 3D cell morphology. These translate into maintained hepatocyte-specific functions and expression of drug metabolic enzymes and drug transporters. Furthermore, hepatocyte spheroids grown in the sponge show inducibility of various drug-metabolizing enzymes including CYP1A2, CYP2B2 and CYP3A1, with higher basal drug-metabolizing expression. The sponge has comparable or lower drug absorbency as other cell culture scaffolds. Importantly, sponge fabrication is amenable for large-scale production and high-throughput screening. Cell seeding into the sponge involves simple steps similar to high-throughput 2D cell cultures. Together, this platform provides a promising tool for hepatocyte-based drug safety testing. As other cells such as stem cells, neuroblasts and cardiomyocytes also show more mature phenotypes when cultured as spheroids, cellulosic sponges may have broad applications in other areas of pharmaceutical research.

Acknowledgement

We thank members of the Cell and Tissue Engineering Laboratory for technical support and stimulating scientific discussions, the Advanced Microscopy Lab at the Biopolis Shared Facilities for their excellent technical assistance in confocal microscopy, Ms. June Ong Lay Ting from IMRE A*STAR for assistance in XPS experiments, Ms. Rashidah bte Sakban for isolating rat hepatocytes and Mr. Abhishek Ananthanarayanan for editing the manuscript. This work is supported in part by funding from the Institute of Bioengineering and Nanotechnology, Biomedical Research Council, Agency for Science, Technology and Research (A*STAR) of Singapore, and grants from Janssen Cilag (R-185-000-182-592), Singapore-MIT Alliance Computational and Systems Biology Flagship Project (C-382-641-001-091), SMART BioSyM and Mechanobiology Institute of Singapore (R-714-001-003-271) to HYU. Bramasta Nugraha is NGS research scholar of the National University of Singapore.

Appendix. Supplementary material

Supplementary video related to this article can be found at doi:10.1016/j.biomaterials.2011.05.087.

References

[1] Smalley KS, Lioni M, Herlyn M. Life isn't flat: taking cancer biology to the next dimension. In Vitro Cell Dev Biol Anim 2006;42(8–9):242–7.
[2] Griffith LG, Swartz MA. Capturing complex 3D tissue physiology in vitro. Nat Rev Mol Cell Biol 2006;7(3):211–24.
[3] Bartosh TJ, Ylostalo JH, Mohammadipoor A, Bazhanov N, Coble K, Claypool K, et al. Aggregation of human mesenchymal stromal cells (MSCs) into 3D spheroids enhances their antiinflammatory properties. Proc Natl Acad Sci U S A 2010;107(31):13724–9.
[4] Fischbach C, Kong HJ, Hsiong SX, Evangelista MB, Yuen W, Mooney DJ. Cancer cell angiogenic capability is regulated by 3D culture and integrin engagement. Proc Natl Acad Sci U S A 2009;106(2):399–404.
[5] Koide N, Sakaguchi K, Koide Y, Asano K, Kawaguchi M, Matsushima H, et al. Formation of multicellular spheroids composed of adult rat hepatocytes in dishes with positively charged surfaces and under other nonadherent environments. Exp Cell Res 1990;186(2):227–35.
[6] Wang S, Nagrath D, Chen PC, Berthiaume F, Yarmush ML. Three-dimensional primary hepatocyte culture in synthetic self-assembling peptide hydrogel. Tissue Eng Part A 2008;14(2):227–36.
[7] Yuasa C, Tomita Y, Shono M, Ishimura K, Ichihara A. Importance of cell aggregation for expression of liver functions and regeneration demonstrated with primary cultured hepatocytes. J Cell Physiol 1993;156(3):522–30.
[8] Abu-Absi SF, Friend JR, Hansen LK, Hu WS. Structural polarity and functional bile canaliculi in rat hepatocyte spheroids. Exp Cell Res 2002;274(1):56–67.
[9] Yamada T, Yoshikawa M, Kanda S, Kato Y, Nakajima Y, Ishizaka S, et al. In vitro differentiation of embryonic stem cells into hepatocyte-like cells identified by cellular uptake of indocyanine green. Stem Cells 2002;20(2):146–54.
[10] Ivascu A, Kubbies M. Rapid generation of single-tumor spheroids for high-throughput cell function and toxicity analysis. J Biomol Screen 2006;11(8):922–32.
[11] Du Y, Chia SM, Han R, Chang S, Tang H, Yu H. 3D hepatocyte monolayer on hybrid RGD/galactose substratum. Biomaterials 2006;27(33):5669–80.
[12] Brophy CM, Luebke-Wheeler JL, Amiot BP, Khan H, Remmel RP, Rinaldo P, et al. Rat hepatocyte spheroids formed by rocked technique maintain differentiated hepatocyte gene expression and function. Hepatology 2009;49(2):578–86.
[13] Takahashi R, Sonoda H, Tabata Y, Hisada A. Formation of hepatocyte spheroids with structural polarity and functional bile canaliculi using nanopillar sheets. Tissue Eng Part A 2010;16(6):1983–95.
[14] Nakazawa K, Izumi Y, Fukuda J, Yasuda T. Hepatocyte spheroid culture on a polydimethylsiloxane chip having microcavities. J Biomater Sci Polym Ed 2006;17(8):859–73.
[15] Yamashita Y, Shimada M, Tsujita E, Tanaka S, Ijima H, Nakazawa K, et al. Polyurethane foam/spheroid culture system using human hepatoblastoma cell line (Hep G2) as a possible new hybrid artificial liver. Cell Transplant 2001;10(8):717–22.
[16] Ijima H, Nakazawa K, Koyama S, Kaneko M, Matsushita T, Gion T, et al. Development of a hybrid artificial liver using a polyurethane foam/hepatocyte-spheroid packed-bed module. Int J Artif Organs 2000;23(6):389–97.
[17] Lee J, Cuddihy MJ, Cater GM, Kotov NA. Engineering liver tissue spheroids with inverted colloidal crystal scaffolds. Biomaterials 2009;30(27):4687–94.
[18] Wells RG. The role of matrix stiffness in regulating cell behavior. Hepatology 2008;47(4):1394–400.
[19] Seglen PO. Preparation of isolated rat liver cells. Methods Cell Biol 1976;13:29–83.
[20] Zhang S, Tong W, Zheng B, Susanto TA, Xia L, Zhang C, et al. A robust high-throughput sandwich cell-based drug screening platform. Biomaterials 2011;32(4):1229–41.
[21] Yue Z, Wen F, Gao S, Ang MY, Pallathadka PK, Liu L, et al. Preparation of three-dimensional interconnected macroporous cellulosic hydrogels for soft tissue engineering. Biomaterials 2010;31(32):8141–52.
[22] Curcio E, Salerno S, Barbieri G, De Bartolo L, Drioli E, Bader A. Mass transfer and metabolic reactions in hepatocyte spheroids cultured in rotating wall gas-permeable membrane system. Biomaterials 2007;28(36):5487–97.
[23] Tostoes RM, Leite SB, Miranda JP, Sousa M, Wang DI, Carrondo MJ, et al. Perfusion of 3D encapsulated hepatocytes–a synergistic effect enhancing long-term functionality in bioreactors. Biotechnol Bioeng 2011;108(1):41–9.
[24] Chang HK, Park YJ, Koh H, Kim SM, Chung KS, Oh JT, et al. Hepatic fibrosis scan for liver stiffness score measurement: a useful preendoscopic screening test for the detection of varices in postoperative patients with biliary atresia. J Pediatr Gastroenterol Nutr 2009;49(3):323–8.
[25] Wang MH, Palmeri ML, Guy CD, Yang L, Hedlund LW, Diehl AM, et al. In vivo quantification of liver stiffness in a rat model of hepatic fibrosis with acoustic radiation force. Ultrasound Med Biol 2009;35(10):1709–21.
[26] Luebke-Wheeler JL, Nedredal G, Yee L, Amiot BP, Nyberg SL. E-cadherin protects primary hepatocyte spheroids from cell death by a caspase-independent mechanism. Cell Transplant 2009;18(12):1281–7.
[27] Harada K, Mitaka T, Miyamoto S, Sugimoto S, Ikeda S, Takeda H, et al. Rapid formation of hepatic organoid in collagen sponge by rat small hepatocytes and hepatic nonparenchymal cells. J Hepatol 2003;39(5):716–23.
[28] Talamini MA, Kappus B, Hubbard A. Repolarization of hepatocytes in culture. Hepatology 1997;25(1):167–72.
[29] Ng S, Han R, Chang S, Ni J, Hunziker W, Goryachev AB, et al. Improved hepatocyte excretory function by immediate presentation of polarity cues. Tissue Eng 2006;12(8):2181–91.
[30] Sidler Pfandler MA, Hochli M, Inderbitzin D, Meier PJ, Stieger B. Small hepatocytes in culture develop polarized transporter expression and differentiation. J Cell Sci 2004;117(Pt 18):4077–87.
[31] Xia L, Ng S, Han R, Tuo X, Xiao G, Leo HL, et al. Laminar-flow immediate-overlay hepatocyte sandwich perfusion system for drug hepatotoxicity testing. Biomaterials 2009;30(30):5927–36.
[32] Nussler AK, Wang A, Neuhaus P, Fischer J, Yuan J, Liu L, et al. The suitability of hepatocyte culture models to study various aspects of drug metabolism. ALTEX 2001;18(2):91–101.
[33] Sakai Y, Yamagami S, Nakazawa K. Comparative analysis of gene expression in rat liver tissue and monolayer- and spheroid-cultured hepatocytes. Cells Tissues Organs 2010;191(4):281–8.
[34] Wolkoff AW, Cohen DE. Bile acid regulation of hepatic physiology: I. Hepatocyte transport of bile acids. Am J Physiol Gastrointest Liver Physiol 2003;284(2):G175–9.
[35] Pang KS, Weiss M, Macheras P. Advanced pharmacokinetic models based on organ clearance, circulatory, and fractal concepts. Aaps J 2007;9(2):E268–83.
[36] Dunn JC, Tompkins RG, Yarmush ML. Hepatocytes in collagen sandwich: evidence for transcriptional and translational regulation. J Cell Biol 1992;116(4):1043–53.
[37] Bokhari M, Carnachan RJ, Cameron NR, Przyborski SA. Novel cell culture device enabling three-dimensional cell growth and improved cell function. Biochem Biophys Res Commun 2007;354(4):1095–100.
[38] Du Y, Han R, Wen F, Ng San San S, Xia L, Wohland T, et al. Synthetic sandwich culture of 3D hepatocyte monolayer. Biomaterials 2008;29(3):290–301.
[39] Zhang S, Xia L, Kang CH, Xiao G, Ong SM, Toh YC, et al. Microfabricated silicon nitride membranes for hepatocyte sandwich culture. Biomaterials 2008;29(29):3993–4002.
[40] Yin C, Liao K, Mao HQ, Leong KW, Zhuo RX, Chan V. Adhesion contact dynamics of HepG2 cells on galactose-immobilized substrates. Biomaterials 2003;24(5):837–50.
[41] Hsiao CC, Wu JR, Wu FJ, Ko WJ, Remmel RP, Hu WS. Receding cytochrome P450 activity in disassembling hepatocyte spheroids. Tissue Eng 1999;5(3):207–21.
[42] Ranucci CS, Kumar A, Batra SP, Moghe PV. Control of hepatocyte function on collagen foams: sizing matrix pores toward selective induction of 2-D and 3-D cellular morphogenesis. Biomaterials 2000;21(8):783–93.
[43] Kim M, Lee JY, Jones CN, Revzin A, Tae G. Heparin-based hydrogel as a matrix for encapsulation and cultivation of primary hepatocytes. Biomaterials 2010;31(13):3596–603.
[44] Green JE, Waters SL, Shakesheff KM, Byrne HM. A mathematical model of liver cell aggregation in vitro. Bull Math Biol 2009;71(4):906–30.
[45] Yoon JJ, Nam YS, Kim JH, Park TG. Surface immobilization of galactose onto aliphatic biodegradable polymers for hepatocyte culture. Biotechnol Bioeng 2002;78(1):1–10.
[46] Nyberg SL, Hardin J, Amiot B, Argikar UA, Remmel RP, Rinaldo P. Rapid, large-scale formation of porcine hepatocyte spheroids in a novel spheroid reservoir bioartificial liver. Liver Transpl 2005;11(8):901–10.
[47] Seo SJ, Choi YJ, Akaike T, Higuchi A, Cho CS. Alginate/galactosylated chitosan/heparin scaffold as a new synthetic extracellular matrix for hepatocytes. Tissue Eng 2006;12(1):33–44.
[48] Chua KN, Lim WS, Zhang P, Lu H, Wen J, Ramakrishna S, et al. Stable immobilization of rat hepatocyte spheroids on galactosylated nanofiber scaffold. Biomaterials 2005;26(15):2537–47.
[49] Feng ZQ, Chu X, Huang NP, Wang T, Wang Y, Shi X, et al. The effect of nanofibrous galactosylated chitosan scaffolds on the formation of rat primary hepatocyte aggregates and the maintenance of liver function. Biomaterials 2009;30(14):2753–63.
[50] Tzanakakis ES, Waxman DJ, Hansen LK, Remmel RP, Hu WS. Long-term enhancement of cytochrome P450 2B1/2 expression in rat hepatocyte spheroids through adenovirus-mediated gene transfer. Cell Biol Toxicol 2002;18(1):13–27.
[51] Padgham CR, Paine AJ, Phillips IR, Shephard EA. Maintenance of total cytochrome P-450 content in rat hepatocyte culture and the abundance of CYP1A2 and CYP2B1/2 mRNAs. Biochem J 1992;285:929–32.
[52] Budinsky RA, LeCluyse EL, Ferguson SS, Rowlands JC, Simon T. Human and rat primary hepatocyte CYP1A1 and 1A2 induction with 2,3,7,8-tetrachlorodibenzo-p-dioxin, 2,3,7,8-tetrachlorodibenzofuran, and 2,3,4,7,8-pentachlorodibenzofuran. Toxicol Sci 2010;118(1):224–35.